VIP Cluster Structures

DOI: 10.1002/anie.201302165

On the Structures of 55-Atom Transition-Metal Clusters and Their Relationship to the Crystalline Bulk**

*Thomas Rapps, Reinhart Ahlrichs, Eugen Waldt, Manfred M. Kappes, and Detlef Schooss**

Surface-immobilized transition-metal clusters (TMC) with particle sizes smaller than 2 nm are assumed to be the active species in many catalytic processes.[1] In this size range 'every atom counts' in determining the properties of the cluster. Consequently, much effort has been invested into experiments under rigorously size-specific conditions. Aside from studies of size-selected TMC on clean surfaces,[2] monodisperse clusters have also been studied in gas-phase.[3] This approach allows substrate and ligand effects to be decoupled from the size-dependent properties of the nanoparticles thus facilitating mechanistic understanding of reactions. A stumbling block remains that structural information is often missing.

To date structural characterizations of free TMC in this size range have mainly been indirect using adsorption site titration[4] or spectroscopic methods[5] coupled with ab initio quantum chemical calculations. Increasingly, trapped-ion electron diffraction (TIED),[6] a more direct structural probe also applicable to larger clusters is being applied. This method is particularly sensitive to the structural motif. While long-established for neutral molecules in the gas-phase, electron diffraction on trapped ions was recently developed to allow measurements on fewer than 10^5 mass-selected particles. Herein, we have used TIED to characterize and compare the structures of a set of homonuclear TMC at constant nuclearity, number of atoms $n = 55$. This size was chosen because with it several closed-shell geometries can be constructed. At this cluster size, a significant fraction of atoms are already bulk rather than surface atoms. Nevertheless, the clusters are still small enough to be treated by density functional theory (DFT). To date theory has only considered a few structural motifs other than the established high-symmetry Mackay icosahedron,[7] truncated decahedron,[8] and cuboctahedron structures—owing to the computational demands of global structure optimization. In most cases 55-atom TMC have just been assumed to be icosahedral—minimizing surface energy while maximizing packing density. As will be shown below this assumption is not always correct.

We used an apparatus described in detail elsewhere[6b] (see also Supporting Information). Briefly, cluster anions were generated by magnetron sputtering, size selected and stored in a quadrupole ion trap held at about 95 K. Thermal equilibrium was reached by collisions with helium atoms. High-energy electrons (40 keV) crossed the trapped ion cloud and scattered electrons were detected on a phosphor screen, yielding the total scattering intensity as function of the scattering angle (represented by electron momentum transfer s). After (atomic) background subtraction, assignment to candidate structures was performed by comparing experimental scattering functions to model simulations (see methods in the Supporting Information). Different structural types exhibit unique experimentally distinguishable fingerprints.

In all cases considered herein, we have determined the structural type. In favorable cases, that is, when there are significant differences between the best and the next-best fit, we have been able to tentatively assign the molecular structure of the cluster.

We have explored M_{55}^- structures for the 3d and 4d elements M = Sc–Cu and Zr–Ag (Y and Tc were not accessible). TIED molecular scattering functions (sM) are shown in Figure 1. Note similarities among the data sets grouped together. Four structure families are discernible: **A**) Sc, Co, Ni, Cu, Pd, Ag (light green), **B**) V, Cr, Mn, Fe, Nb, Mo (light blue), **C**) Ti, Zr (light red) and **D**) Ru and Rh (dark green). Note also the periodic trends in average bond lengths which are evident from the positions of the corresponding diffraction maxima (vertical arrows). Small variations in the molecular scattering function within a structure family are due to different element-specific isomers of the same structure type.

Structural models were obtained from a combination of semi-empirical and quantum-chemical calculations. Candidate structures were sought in an automated multi-step procedure. Global optimization based solely on ab initio methods (i.e. genetic algorithm (GA) + DFT), is still prohibitive for clusters of this size. Instead, we used a GA search based on empirical potentials parameterized for different transition metals (TM) to find low energy structures. Additionally, a modified GA also including TIED data was used for appraising trial structures.[9] Lowest energy and best-fitting structures were then further optimized using DFT with a generalized gradient functional[10]—in the program system TURBOMOLE[11] with split valence polarization basis sets.[12] Further details about the empirical metal potentials and the

[*] Dr. T. Rapps, Prof. Dr. R. Ahlrichs, E. Waldt, Prof. Dr. M. M. Kappes, Dr. D. Schooss
Institut für Nanotechnologie
Karlsruher Institut für Technologie (KIT)
Karlsruhe (Germany)
E-mail: detlef.schooss@kit.edu
Prof. Dr. R. Ahlrichs, Prof. Dr. M. M. Kappes, Dr. D. Schooss
Institute für Physikalische Chemie
Karlsruher Institut für Technologie (KIT)
Karlsruhe (Germany)

[**] This research was supported by BMBF through the Helmholtz Research Program POF NanoMikro and by DFG through the Center for Functional Nanostructures (TP4.6). R.A. and M.M.K. also acknowledge support by Fonds der Chemischen Industrie.

Supporting information for this article is available on the WWW under http://dx.doi.org/10.1002/anie.201302165.

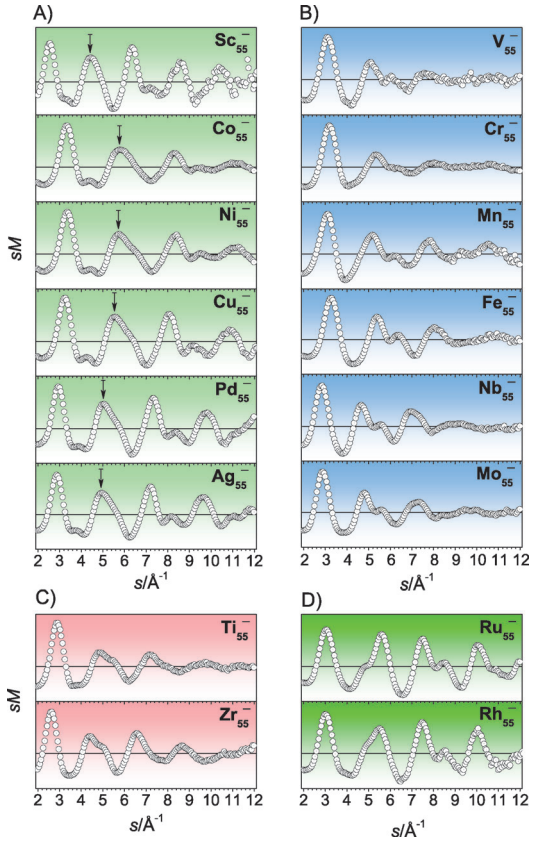

Figure 1. Experimental molecular scattering functions *sM* of M_{55}^- cluster ions of the 3d and 4d elements M = Sc–Cu, Zr–Ag (without Tc) correspond to only four different structural families (**A**–**D**). Element specific differences in average bond lengths lead to scaling of the momentum transfer axis *s* (vertical arrows mark characteristic corresponding positions).

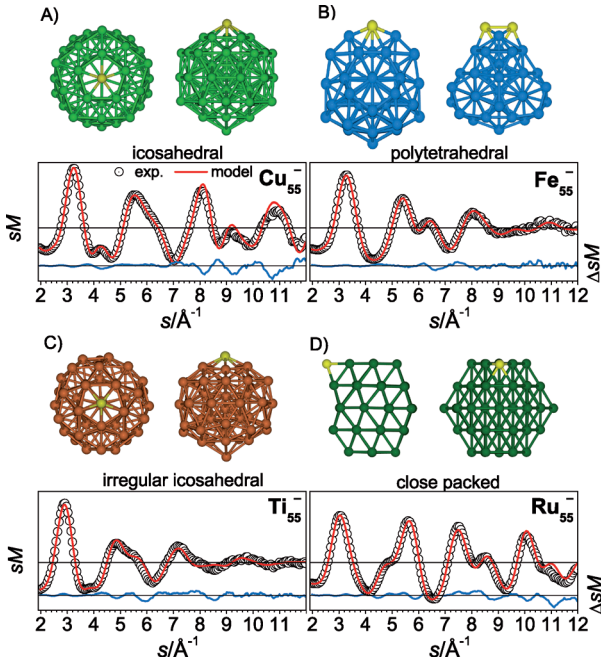

Figure 2. Experimental (open circles) and simulated (red line) molecular scattering functions *sM* for the best fitting candidate structures of Cu_{55}^-, Fe_{55}^-, Ti_{55}^-, and Ru_{55}^-. Shown in the lower part are residual ΔsM values (blue line) to the same scale. Above each fit are two views of the corresponding clusters their relative orientation being indicated by yellow atoms. The clusters shown are prototypical examples of each of the four structure families (**A**–**D**).

DFT method used are given in the methods section of the Supporting Information.

Figure 2 shows the best-fitting candidate structures for examples chosen from each of the four structure families: **A**) Cu_{55}^-, **B**) Fe_{55}^-, **C**) Ti_{55}^-, and **D**) Ru_{55}^-. Additionally, we document the quality of the fits by contrasting them with the experimental data. Generally, experimental and theoretical scattering functions were compared using a χ^2 analysis including parameterizations for thermal vibrations and experimental broadening. An overview of the best fits obtained for all the TMC studied and typical results of the fitting procedure which contrasts different structural candidates are given in the Supporting Information Figure S1 and Figures S3–S6.

The lowest energy isomers considered in DFT calculations always provide the best or close to the best agreement with measurement. This implies that: 1) the level of DFT calculation used provides total energy accuracy to within several tenths of an electron volt and 2) the experiment probes lowest (free) energy forms rather than kinetically trapped isomer distributions. Consistent with previous work on other cluster systems, we generally fit each experimental data set with a single model structure—resulting in good agreement.[13] Only for Rh_{55}^- was it necessary to model the measurement in terms of a superposition of two structure types (**D** + **A**, see Figure S2).

Next we discuss major structural features of each family. Cu_{55}^- belongs to group **A** together with Sc_{55}^-, Co_{55}^-, Ni_{55}^-, Pd_{55}^-, and Ag_{55}^-. All have high-symmetry icosahedral structures—the 55-atom closed-shell Mackay icosahedra[7] consisting of shells of 12 and 42 atoms around a central atom. Group **A** structures can also be considered as multiply twinned particles (MTP) composed of 20 tetrahedra stacked in an fcc fashion. This arrangement is not space-filling and leads to a gap of approximately 7.4° when five regular tetrahedra are packed around a common edge. In the actual relaxed structures, this causes bond-length variations: intra-shell separations become larger towards the surface, while inter-shell separations decrease.

Owing to the overall icosahedral symmetry, however, the local structure remains very regular. As a result, edge and corner atoms have coordination numbers (CN) of 6 and 8, respectively, whereas all the bulk atoms have CN 12.

Most group **A** clusters show either full I_h symmetry or only small Jahn–Teller distortions. Pd_{55}^- is an exception. It relaxes significantly into a C_i symmetry structure with a maximum relative bond-length deviation of approximately 0.5 % from I_h. Even within full I_h symmetry, a 55-atom cluster has (three) freely variable structural parameters. Small corresponding variations are seen for (bulk) fcc and hcp elements (see also *sM* functions in Figure 1): Ni_{55}^-, Cu_{55}^-, and Ag_{55}^- prefer typical MTP geometries with sphere-like structures featuring rounded corners and edges. In contrast, Co_{55}^-

forms almost planar facets as in a regular Platonic icosahedron. Sc_{55}^-, the second hcp element in this group, has remarkably long bonds, especially between the central atom and its surrounding shell.

Family **B** (V_{55}^-, Cr_{55}^-, Mn_{55}^-, Fe_{55}^-, Nb_{55}^-, and Mo_{55}^-) is polytetrahedral[14] with subsurface atoms forming locally—but not globally—icosahedral coordination shells. Similar to Mackay icosahedra, polytetrahedral packing of atoms can become increasingly frustrated leading to larger surface strains. The Fe_{55}^- structure (Figure 2) can be described by four interpenetrating 19-atom double icosahedra. This leads to reduced sphericity compared to an icosahedron and higher numbers of surface atoms. Similar to Frank–Kasper phases (quasicrystals or metallic glasses),[15] the strain of polytetrahedral packing is reduced by adding polyhedrons having high local coordination numbers (up to CN 16). This arrangement leads to a mean CN of 8.91, which is significantly larger than for class **A** (8.51), thus more than compensating for low-coordinate surface atoms. Incorporation of high CN polyhedra also leads to larger bond-length variances than for icosahedra (relative standard variation 5.3% for Fe_{55}^- versus 2.4% for Cu_{55}^-, see also Table S1 and S2 in the Supporting Information) resulting in increased damping of the molecular scattering function. Different group **B** elements have different best-fitting isomers—within the same structure type. The polytetrahedral motif allows a wide range of isomers within small energy intervals (ca. 1 eV). These have very similar molecular scattering functions and therefore the global minimum may not have been found for each element of this group. Similarly, mixtures of several polytetrahedral isomers cannot be ruled out.

The hcp TM elements titanium and zirconium constitute family **C**. Ti_{55}^-, Zr_{55}^- have irregular icosahedral geometries. Fairly spherical with some resemblance to Mackay icosahedra, they have low overall symmetry (Ti_{55}^-: C_1). The structures can be understood as hybrids of types **A** and **B**. In comparison to type **A**, internal and surface atoms are rearranged to yield a higher mean coordination number (8.73). In contrast to type **B**, an increased coordination of internal atoms is not the only factor determining geometries. In this case minimization of surface energy, as manifested by a lower number of surface atoms and more-spherical shapes, is also important.

Type **D**, as found for Ru_{55}^- and Rh_{55}^-, comprises close packed geometries resembling segments of the fcc or hcp bulk. Best fitting models manifest "stacking faults" in their hexagonal sheet ordering (ABCBA rather than ABCAB—fcc or ABABA—hcp). In comparison to a regularly fcc-stacked, closed-shell cuboctahedron (O_h), such "stacking faults" reduce particle surface area and yield a lower ratio of open high energy (100) to compact (111) facets. In Ru_{55}^- this effect leads to a 4.2 eV stabilization. At only 1.8%, the bond-length variation is significantly smaller than for structure families **A**–**C**. The mean CN is only 8.0 and the CN never exceeds 12. Apparently, there is a high energy penalty for significant bond-length variations relative to bulk. The high rigidity of the underlying potential compensates for the lower CN. For Rh_{55}^- a mixture two different structural types (**A** + **D**) is found by experiment. The icosahedral-to-bulk structure transition apparently already occurs in the 55 atom size-range. Note, that among the free TMC studied herein, bulk-like structures have never been inferred for such small particles sizes.

TM bulk structures alternate regularly in the order hcp → bcc → hcp → fcc (see Figure 3) upon traversing the periodic table from left to right. Interestingly, free cluster structure types generally correlate with these bulk lattice types. All

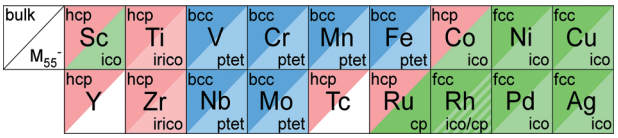

Figure 3. 3d and 4d transition-metal-element bulk lattice types under standard conditions (top left corner) with the corresponding gas-phase structure types of M_{55}^- at 95 K (bottom right corner). Correlation is indicated by (the same) light and dark color : hcp/irregular icosahedral (irico, red), bcc/polytetrahedral (ptet, blue), fcc/icosahedral (ico, light green) and fcc/close packed (cp, dark green).

bulk fcc elements form icosahedral clusters (or for Rh_{55}^- an **A** + **D** mixture). All bcc elements form polytetrahedral clusters. Only hcp elements show more nuanced behavior. The early hcp elements Ti and Zr belong to the irregular icosahedral family. The late hcp elements Co and Ru behave differently. Ru_{55}^- already has a bulk-like structure. The icosahedral structure type of Co_{55}^- may be rationalized in terms of the high temperature (> 427 °C) bulk β-Co fcc modification—indicating that hcp and fcc bulk structures are close in energy. The only real exception to the structural correlation is the early hcp element scandium.

For those M_{55}^- ions in which the bulk structure is not yet realized, the maximum CN of internal atoms as well as their mean CN increases in the sequence icosahedral → irregular icosahedral → polytetrahedral. Mackay icosahedra have solely CN 12 with small bond-length variances. Besides having icosahedral sites (CN 12), polytetrahedral clusters comprise highly coordinated atoms with up to CN 16 (accompanied by a bond-length variation of 5.3–7.6%). Again this property correlates with the corresponding bulk lattices: the CN is 12 in fcc/hcp and 8 + 6 in bcc (8 nearest neighbors are raised to 14 if the next-nearest neighbors in the connected primitive cells are also included, corresponding to an elongated bond length of ca. 15%).

Electron-configuration-dependent effective interatomic potentials in TM elements differ qualitatively in how they respond to deviations from optimal bond lengths, for example, as evident in the occurrence of bcc versus fcc elements. In clusters this dependence leads to different types of nanostructures—reflecting an interplay between maximization of the average CN and minimization of the surface-energy. Highly rigid effective potentials, such as in Ru and Rh, lead to strain-free bulk-like structures in which surface-energy destabilization can be more than compensated.

In summary, we have observed a general correlation of TM cluster structure type with bulk lattice morphology (under standard conditions). This remarkably simple rule is valid for most 3d and 4d TM elements. Our finding is relevant

to the largely unsolved problem of predicting the structure of crystalline TM solids.[16] Knowledge of periodic trends in elemental morphology at the nanoscale may be of help.

Received: March 14, 2013
Published online: May 9, 2013

Keywords: cluster structure · electron diffraction · structure elucidation · transition metals · TIED

[1] A. S. K. Hashmi, G. J. Hutchings, *Angew. Chem.* **2006**, *118*, 8064 – 8105; *Angew. Chem. Int. Ed.* **2006**, *45*, 7896 – 7936.
[2] a) Z. Y. Li, N. P. Young, M. Di Vece, S. Palomba, R. E. Palmer, A. L. Bleloch, B. C. Curley, R. L. Johnston, J. Jiang, J. Yuan, *Nature* **2008**, *451*, 46 – 48; b) B. Yoon, H. Häkkinen, U. Landman, A. S. Worz, J. M. Antonietti, S. Abbet, K. Judai, U. Heiz, *Science* **2005**, *307*, 403 – 407; c) W. E. Kaden, T. Wu, W. A. Kunkel, S. L. Anderson, *Science* **2009**, *326*, 826 – 829; d) H.-J. Freund, G. Pacchioni, *Chem. Soc. Rev.* **2008**, *37*, 2224 – 2242.
[3] a) M. D. Morse, M. E. Geusic, J. R. Heath, R. E. Smalley, *J. Chem. Phys.* **1985**, *83*, 2293 – 2304; b) D. J. Trevor, R. L. Whetten, D. M. Cox, A. Kaldor, *J. Am. Chem. Soc.* **1985**, *107*, 518 – 519.
[4] E. K. Parks, B. J. Winter, T. D. Klots, S. J. Riley, *J. Chem. Phys.* **1991**, *94*, 1882 – 1902.
[5] a) J. Li, X. Li, H.-J. Zhai, L.-S. Wang, *Science* **2003**, *299*, 864 – 867; b) P. Gruene, D. M. Rayner, B. Redlich, A. F. G. van der Meer, J. T. Lyon, G. Meijer, A. Fielicke, *Science* **2008**, *321*, 674 – 676.
[6] a) M. Maier-Borst, D. B. Cameron, M. Rokni, J. H. Parks, *Phys. Rev. A* **1999**, *59*, R3162 – R3165; b) D. Schooss, M. N. Blom, J. H. Parks, B. von Issendorff, H. Haberland, M. M. Kappes, *Nano Lett.* **2005**, *5*, 1972 – 1977.
[7] A. L. Mackay, *Acta Crystallogr.* **1962**, *15*, 916 – 918.
[8] S. Ino, *J. Phys. Soc. Jpn.* **1969**, *27*, 941 – 953.
[9] C. Neiss, D. Schooss, *Chem. Phys. Lett.* **2012**, *532*, 119 – 123.
[10] a) A. D. Becke, *Phys. Rev. A* **1988**, *38*, 3098 – 3100; b) J. P. Perdew, *Phys. Rev. B* **1986**, *33*, 8822; c) J. P. Perdew, *Phys. Rev. B* **1986**, *34*, 7406 – 7406.
[11] R. Ahlrichs, M. Bär, M. Häser, H. Horn, C. Kölmel, *Chem. Phys. Lett.* **1989**, *162*, 165 – 169.
[12] TURBOMOLE basis set library II, http://www.cosmologic.de/basis-sets/basissets.php, (**2012**).
[13] a) M. N. Blom, D. Schooss, J. Stairs, M. M. Kappes, *J. Chem. Phys.* **2006**, *124*, 244308; b) A. Lechtken, D. Schooss, J. R. Stairs, M. N. Blom, F. Furche, N. Morgner, O. Kostko, B. von Issendorff, M. M. Kappes, *Angew. Chem.* **2007**, *119*, 3002 – 3006; *Angew. Chem. Int. Ed.* **2007**, *46*, 2944 – 2948; c) D. Schooss, P. Weis, O. Hampe, M. M. Kappes, *Philos. Trans. R. Soc. London Ser. A* **2010**, *368*, 1211 – 1243.
[14] a) J. P. K. Doye, D. J. Wales, *Phys. Rev. Lett.* **2001**, *86*, 5719 – 5722; b) J. A. Elliott, Y. Shibuta, D. J. Wales, *Philos. Mag.* **2009**, *89*, 3311 – 3332.
[15] F. C. Frank, J. S. Kasper, *Acta Crystallographica* **1958**, *11*, 184 – 190.
[16] J. Maddox, *Nature* **1988**, *335*, 201.

